Check for updates

Europe
European Chemical
Societies Publishing

▌Medicinal Chemistry │Hot Paper│

MUC1 Aptamer-Capped Mesoporous Silica Nanoparticles for Navitoclax Resistance Overcoming in Triple-Negative Breast Cancer

Gema Vivo-Llorca,[a, b, e] Vicente Candela-Noguera,[a, b] María Alfonso,[a, b] Alba García-Fernández,[a, b, c, e] Mar Orzáez,*[e, f] Félix Sancenón,*[a, b, c, d, e] and Ramón Martínez-Máñez*[a, b, c, d, e]

Abstract: Triple-negative breast cancer (TNBC) is the most aggressive breast cancer subtype. In the last years, navitoclax has emerged as a possible treatment for TNBC. Nevertheless, rapid navitoclax resistance onset has been observed thorough Mcl-1 overexpression. As a strategy to overcome Mcl-1-mediated resistance, herein we present a controlled drug co-delivery system based on mesoporous silica nanoparticles (MSNs) targeted to TNBC cells. The nanocarrier is loaded with navitoclax and the Mcl-1 inhibitor S63845 and capped with a MUC1-targeting aptamer (**apMUC1-MSNs(Nav/S63845)**). The apMUC1-capped nanoparticles effectively target TNBC cell lines and successfully induce apoptosis, overcoming navitoclax resistance. Moreover, navitoclax encapsulation protects platelets against apoptosis. These results point apMUC1-gated MSNs as suitable BH3 mimetics nanocarriers in the targeted treatment of MUC1-expressing TNBC.

Introduction

Breast cancer is the most frequently diagnosed and the leading cause of cancer death in women worldwide.[1,2] Among breast

[a] G. Vivo-Llorca, V. Candela-Noguera, Dr. M. Alfonso, Dr. A. García-Fernández, Dr. F. Sancenón, Prof. R. Martínez-Máñez
Instituto Interuniversitario de Investigación de Reconocimiento Molecular y Desarrollo Tecnológico (IDM), Universitat Politècnica de València
València (Spain)
E-mail: fsanceno@upvnet.upv.es

[b] G. Vivo-Llorca, V. Candela-Noguera, Dr. M. Alfonso, Dr. A. García-Fernández, Dr. F. Sancenón, Prof. R. Martínez-Máñez
Departamento de Química, Universitat Politècnica de València
Camino de Vera s/n, 46022 Valencia (Spain)
E-mail: rmaez@qim.es

[c] Dr. A. García-Fernández, Dr. F. Sancenón, Prof. R. Martínez-Máñez
CIBER de Bioingeniería, Biomateriales y Nanomedicina (CIBER-BBN)
Madrid (Spain)

[d] Dr. F. Sancenón, Prof. R. Martínez-Máñez
Unidad Mixta de Investigación en Nanomedicina y Sensores
Universitat Politècnica de València, IIS La Fe, Valencia (Spain)

[e] G. Vivo-Llorca, Dr. A. García-Fernández, Prof. M. Orzáez, Dr. F. Sancenón, Prof. R. Martínez-Máñez
Unidad Mixta UPV-CIPF de Investigación en Mecanismos de Enfermedades y Nanomedicina, Universitat Politècnica de València y Centro de, Investigación Príncipe Felipe, València (Spain)

[f] Prof. M. Orzáez
Centro de Investigación Príncipe Felipe
Eduardo Primo Yúfera, 3, Valencia 46012 (Spain)
E-mail: morzaez@cipf.es

Supporting information and the ORCID identification number(s) for the author(s) of this article can be found under:
https://doi.org/10.1002/chem.202001579.

cancers (BCs), triple-negative breast cancer (TNBC) accounts for approximately 15–20 % of breast carcinomas.[3] Moreover, TNBC shows the poorest outcome due to its aggressiveness, chemotherapy resistance, early recurrence and high risk of metastasis.[4] TNBC is defined by the lack of the three main breast cancer biomarkers, that is, estrogen, progesterone, and HER2 receptors.[5] Due to the loss of such receptors, TNBC patients do not respond to targeted treatments (endocrine or anti-HER2 therapy), and first-line treatment of TNBC patients is chemotherapy combined with surgery and/or radiotherapy. This scenario warrants the need for the development of new strategies to treat TNBC.[6,7]

Evasion of apoptosis is a hallmark of cancer.[8] The proteins from BCL-2 family are the key mediators of this type of cell death. They are divided into three subfamilies: the pro-apoptotic BH3-only ligands (BID, BAD, BIM, PUMA, NOXA, etc.), the pro-apoptotic multi-BH domain effector proteins (BAX and BAK) and the antiapoptotic proteins (Bcl-2, Bcl-xL, Bcl-w, Mcl-1, and Bfl-1).[9–11] The balance between proapoptotic and antiapoptotic members determines cell survival or death. In the case of tumors, this equilibrium often leans towards survival, leading to sustained tumor expansion and chemotherapy resistance.[12] To overcome this tumor survival mechanism, several inhibitors of BCL-2 antiapoptotic proteins, also called BH3 mimetic drugs, such as ABT-263 (known as navitoclax) have been developed.[13] In fact, navitoclax is currently involved in several clinical trials on different solid and liquid tumors (NCT01989585 NCT02520778, NCT03181126, NCT03366103, NCT03222609 and NCT02079740).[14]

Chemistry–A European Journal

Full Paper
doi.org/10.1002/chem.202001579

**Chemistry
Europe**
European Chemical
Societies Publishing

From these clinical trials, it became apparent that there are two main limitations to the use of navitoclax. First, some side effects in patients, from which the most relevant is thrombocytopenia, as a consequence of platelets dependence on Bcl-xL for survival, which makes platelets especially sensitive to navitoclax.[15] A second drawback is that navitoclax targets only three antiapoptotic members of the BCL-2 protein family (i.e., Bcl-w, Bcl-2, and Bcl-xL), but it does not target the antiapoptotic protein Mcl-1. This leads to the rapid development of treatment resistance in cancer cells thorough Mcl-1 overexpression.[13,16] Mcl-1 overexpression has been associated with a bad prognosis in BC patients.[16,17] Recently, a highly specific Mcl-1 inhibitor, named S63845, has been developed and its antiproliferative activity has been demonstrated in several malignancies in vitro and in vivo.[18] In this scenario, the synergistic action of the Mcl-1 inhibitor S63845 and BH3 mimetic drugs against BCs and other cancers has been reported.[19,20]

One of the main strategies to reduce drug side effects is the use of nanocarriers. This is, for instance, exemplified in the drug Doxil; a nanoformulated form of doxorubicin approved by the FDA in 1995, which shows reduced cardiotoxicity when compared with the free drug.[21,22] Moreover, nanoparticles have been reported to accumulate in tumors by the enhanced permeability and retention (EPR) effect.[23–25] This EPR effect, together with the possibility of delivering a specific drug on-command, make nanoparticles suitable systems to increase the on-target therapeutic effect while diminishing side effects.[23,26–28]

Among different reported nanocarriers, mesoporous silica nanoparticles (MSNs) have been widely used as drug delivery systems to treat several malignancies.[23,26,29,30] MSNs highlight in the biomedical investigation due to their properties, such as large specific volume and area, homogeneous pore size, highly stable structure, biocompatibility, and easy surface functionalization.[27,31–34] However, the most appealing feature of MSNs as nanocarriers is the possibility of designing gated materials for the on-command release of drugs, in which MSNs outer surface is functionalized with (bio)molecules that prevent payload release unless the drug-loading system is exposed to specific stimuli.[35–41] Such gated MSNs have been applied as suitable systems for drug delivery, sensing and communication applications.[35,40,42] Additionally, MSNs can be functionalized with targeting ligands.[23,28] Among them, aptamers have been extensively used to develop targeted materials for biomedical applications.[43–47] Aptamers are short single-strand DNA or RNA oligonucleotides that fold into 3D structures that bind and target molecules with high affinity and specificity. To develop active nanocarriers with targeting abilities, a common approach is to target surface receptors overexpressed in selected cells.[48–51] In this scenario and concerning BCs, MUC1 is a transmembrane glycoprotein belonging to the mucin family, which is aberrantly overexpressed in 70% of BCs and it has been recognized as an important molecular target in cancer.[26,52,53]

Based on the above-mentioned facts, we were interested in designing nanoparticles for their potential enhanced use in the treatment of BCs. Specifically, we focused our attention on the preparation of nanoparticles that could overcome the two lim-
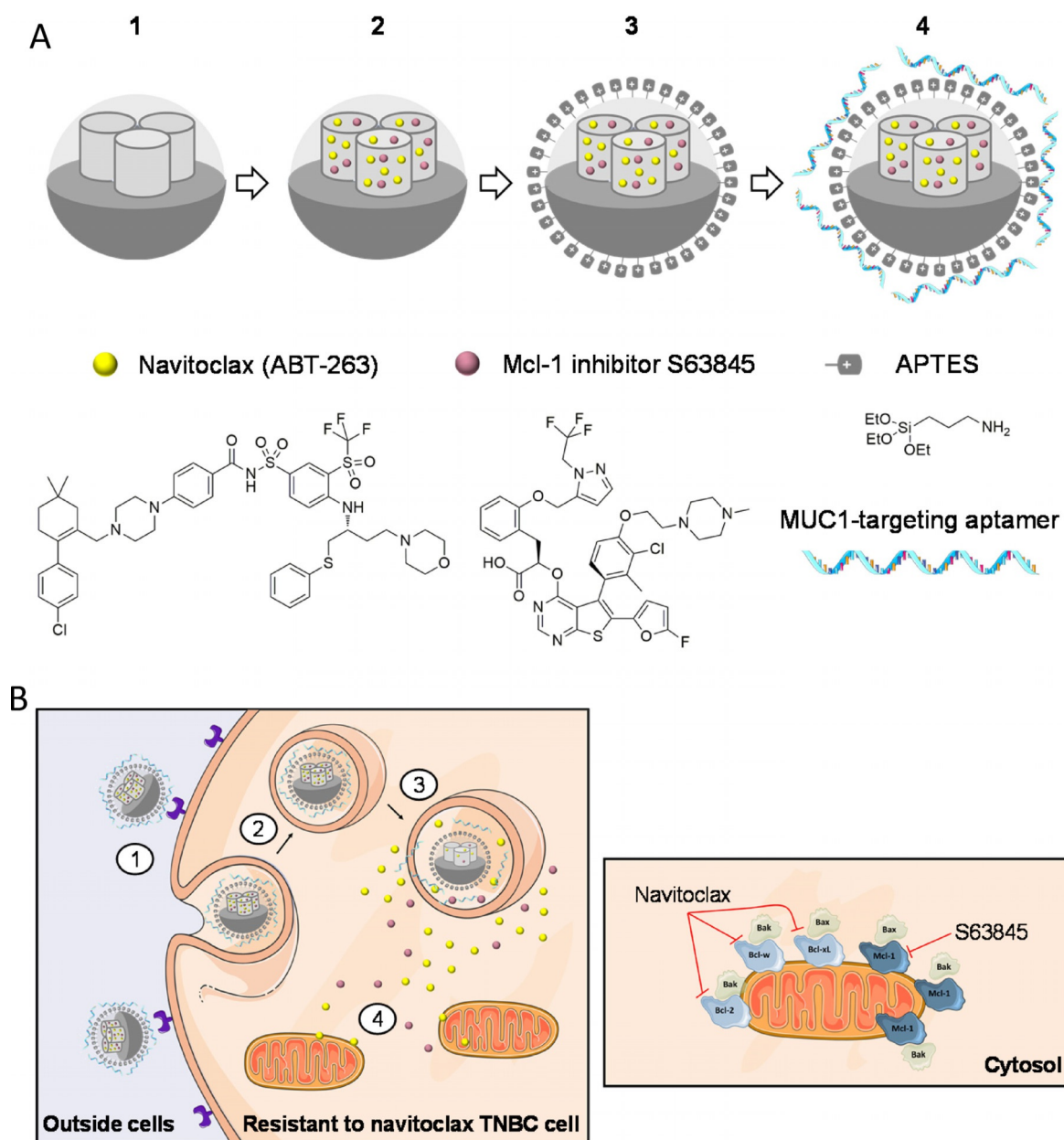
iting properties of navitoclax as a drug: that is, platelet toxicity and resistances through Mcl-1 overexpression. With this aim, we prepare herein MSNs loaded with navitoclax and the Mcl-1 inhibitor S63845, and capped with an aptamer (apMUC1) targeting the MUC1 surface protein overexpressed in TNBC (**apMUC1-MSNs(Nav/S63845)**). We demonstrate the enhanced antitumoral activity of the nanoparticles **apMUC1-MSNs(Nav/S63845)** and their active targeting to TNBC cells. We also show that navitoclax encapsulation in MSNs reduces thrombocytopenia in human blood samples, which is its principal dose-limiting effect. These promising results point MSNs as useful nanocarriers of drugs to overcome drug resistance and drug side effects in TNBC.

Results and Discussion

Synthesis and characterization of aptamer-capped nanoparticles

For the synthesis of apMUC1-gated nanodevices, we used MSNs and loaded them with different cargos (vide infra and Table S1). After the loading process, the nanoparticles were functionalized with (3-aminopropyl) triethoxysilane (APTES). This gave nanoparticles externally functionalized with amino groups. Amino groups are partially protonated at neutral pH and are known to give strong electrostatic and hydrogen bonding interactions with aptamers such as the MUC1 aptamer (i.e., 5-GCA GTT GAT CCT TTG GAT ACC CTG G-3'), which was used to cap the pores. This procedure yielded the nanoparticles **apMUC1-MSNs(RhB)**, **apMUC1-MSNs(Nav)**, **apMUC1-MSNs(S63845)**, in which the apMUC1-capped MSNs are loaded with the fluorescent rhodamine B dye, navitoclax, and the Mcl-1 inhibitor S63845, respectively. Moreover, apMUC1-capped MSNs were also simultaneously loaded with navitoclax and S63845 using two different molar ratios to give the nanoparticles **apMUC1-MSNs(Nav/S63845, 10:1)** and **MSNs(Nav/S63845, 2:1)**, respectively (Scheme 1A). For biocompatibility studies, empty MSNs were functionalized with APTES and capped with apMUC1 (**apMUC1-MSNs**). Additionally, control nanoparticles loaded with rhodamine B, functionalized with APTES and capped with a random aptamer were also synthesized (**apRandom-MSNs(RhB)**). The designed nanodevices are expected to be endocytosed after interaction between the MUC1 aptamer and the overexpressed MUC1 receptor in the membrane of TNBC cells, resulting in nanoparticles' internalization and cargo delivery inside cells. Delivery of navitoclax and the Mcl-1 inhibitor S63845 is expected to neutralize BCL-2 antiapoptotic proteins, leading to tumor cell death by apoptosis (Scheme 1B).

The prepared nanoparticles were characterized using powder X-ray diffraction (PXRD), N_2 adsorption–desorption isotherms, Fourier-transform infrared spectroscopy (FTIR), transmission electron microscopy (TEM), transmission electron microscopy coupled with energy-dispersive X-ray spectroscopy (TEM-EDX) and ζ potential. The PXRD pattern of calcined MSNs is typical for mesoporous silica materials with low-angle peaks characteristic of a hexagonal-ordered pore array. The preserva-

Chemistry–A European Journal

Full Paper
doi.org/10.1002/chem.202001579

Chemistry
Europe
European Chemical
Societies Publishing

Scheme 1. A) Scheme of mesoporous silica nanoparticles (MSNs) (1) loaded with navitoclax and the Mcl-1 inhibitor S63845 (2), functionalized with APTES (3) and capped with the MUC1-targeting aptamer (4). B) Scheme of the mechanism of action of **apMUC1-MSNs(Nav/S63845)**. After the interaction of the MUC1-targeting aptamer with the MUC1 surface protein (1), MSNs endocytosis takes place (2) and nanoparticles reach the lysosome (3). Drugs are released from the nanoparticles and they reach their target proteins in the mitochondria (4): that is, navitoclax targets Bcl-2, Bcl-w and Bcl-xL and S63845 targets Mcl-1. The inhibition of BCL-2 antiapoptotic set of proteins triggers apoptosis by bax/bak oligomerization in the mitochondria membrane.

tion of the (100) reflection demonstrated that loading and functionalization processes with APTES did not damage the mesoporous structure in the nanoparticles (see for instance the PXRD pattern of **APTES-MSNs(RhB)** in Figure S1A). The FTIR spectrum of **APTES-MSNs(RhB)** showed symmetric and asymmetric stretching N-H and C—H bands from APTES within the 3100–2840 cm^{-1} range, whereas nanoparticle capped with the MUC1 aptamer, additionally, showed vibrations of the nucleobases (C=O, C=N, C=C and C–C bonds) in the 1750–1550 cm^{-1} range (Figure S1B).[54,55] The N$_2$ adsorption–desorption isotherms of the starting MSNs (Figure S1C) showed the

typical type IV isotherm with a specific surface area of 1088 m^{2}g^{-1}, by applying the Brunauer–Emmett–Teller (BET) model, and a pore volume and pore diameter of 0.73 cm^{3}g^{-1} and 3.31 nm, respectively, by using the density functional theory (DFT) method on the adsorption branch of the isotherm. In contrast, N$_2$ adsorption–desorption isotherm of **APTES-MSNs(RhB)** was typical of mesoporous systems with partially filled mesopores, with a reduced specific surface area (203 m^{2}g^{-1}) and pore volume (0.13 cm^{3}g^{-1}). We also monitored the different steps of the preparation of the final nanocarriers by hydrodynamic diameter using dynamic light scattering

Chemistry–A European Journal

Full Paper
doi.org/10.1002/chem.202001579

Chemistry Europe
European Chemical
Societies Publishing

(DLS) and ζ potential (Table S2). The hydrodynamic diameter increased after each preparation step. The starting calcined nanoparticles presented a hydrodynamic diameter of 173(± 1.3) nm. The functionalization of the drug-loaded nanoparticles with APTES resulted in an increase of the hydrodynamic size (to ca. 200 nm) and the subsequent capping with apMUC1 yield nanoparticles with a hydrodynamic diameter of about 500 nm (Table S2). We also monitored the different steps of the preparation of the final nanocarriers by ζ potential. Calcined MCM-41 nanoparticles presented a ζ potential of −27(± 2) mV (due to the presence of silanolate moieties onto its external surface) which changed to positive values after loading and functionalization with APTES (due to the amino groups). After capping with the MUC1 aptamer, ζ potential shifted back to negative, indicating the successful incorporation of the oligonucleotide into the final nanodevices (Table S2).

TEM images of the starting MSNs showed spherical nanoparticles (average size of ca. 100 nm) and the presence of alternated black and white stripes, typical of mesoporous systems (Figure S2A). The same morphology and similar size were observed for the intermediate (APTES-functionalized nanoparticles) (Figure S2B) and the final apMUC1-capped solids (Figure S2C), confirming the preservation of the mesoporous structure during the functionalization process. Furthermore, TEM-EDX mapping studies were performed. As an example, Figure 1A shows TEM-EDX images of **apMUC1-MSNs(Nav/S63845, 10:1)**, that clearly demonstrated the presence of Si and O (from the silica scaffold), F and S (from the cargoes), N (from APTES and apMUC1) and P (from apMUC1), which indicates the correct loading with the drugs (i.e., navitoclax and S63845), the presence of APTES and the capping apMUC1 aptamer.

Moreover, drug loading and the aminopropyl and apMUC1 contents in the nanoparticles were determined by thermogravimetric studies, elemental analyses and ^{1}H NMR upon forced cargo delivery in ethanol. The amount of navitoclax and S63845 in **apMUC1-MSNs(Nav)** and **apMUC1-MSNs(S63845)** was quantified as 97.5 µmol g^{-1} and 102.0 µmol g^{-1}, respectively. The amount of drugs in **apMUC1-MSNs(Nav/S63845, 10:1)** was determined as 106.9 µmol g^{-1} of navitoclax and 11.9 µmol g^{-1} of S63845, and in **apMUC1-MSNs(Nav/S63845, 2:1)** as 60.3 µmol g^{-1} of navitoclax and 31.9 µmol g^{-1} of S63845 per mg of MSNs, which is consistent with the navitoclax/
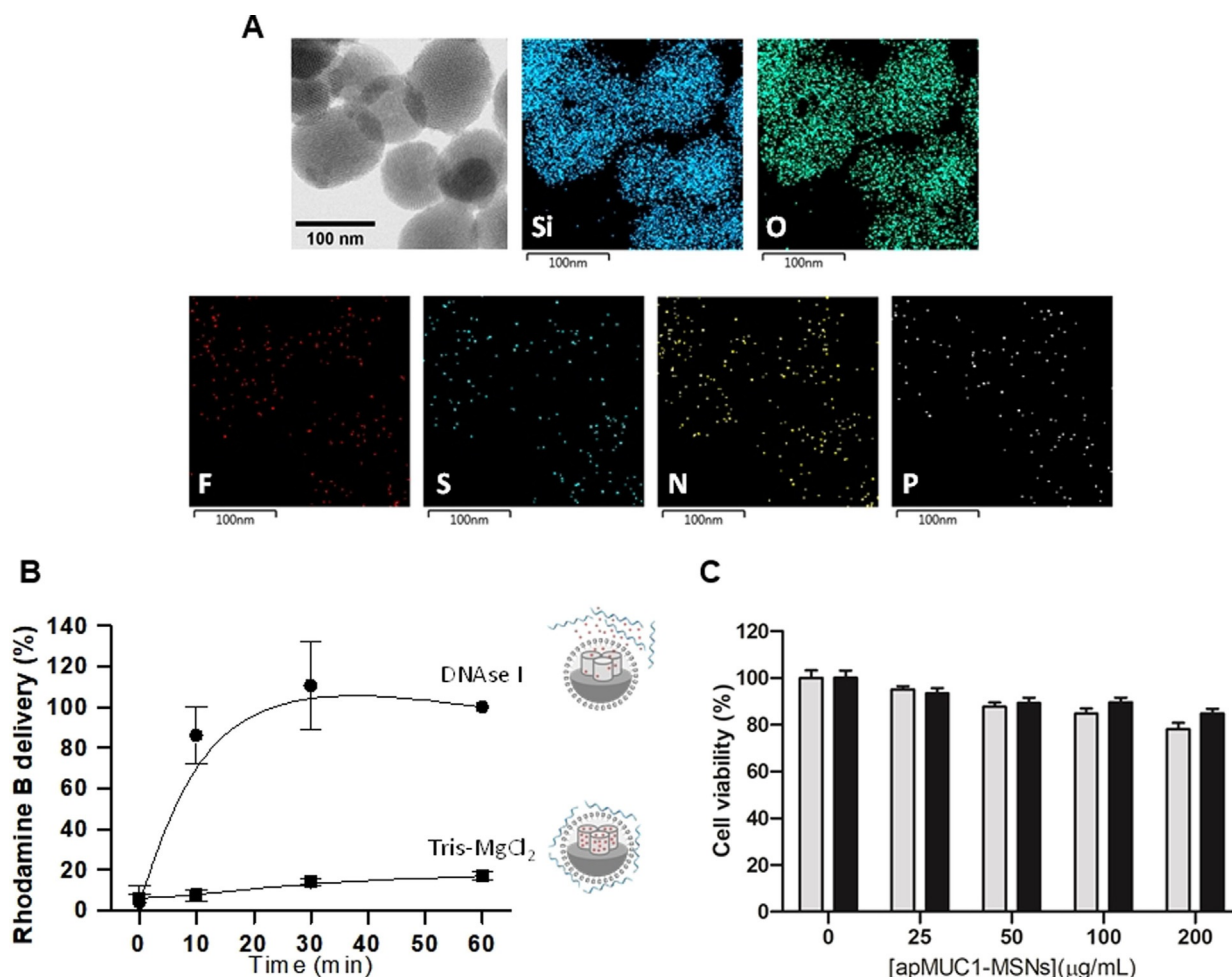

Figure 1. A) TEM-EDX map for **apMUC1-MSNs(Nav/S63845, 10:1)** showing the presence of Si and O (from the silica scaffold), F and S (from the cargoes), N (from APTES and apMUC1) and P (from apMUC1). B) Release profile of rhodamine B from **apMUC1-MSNs(RhB)** in the absence (bottom) and presence (top) of DNAse I. C) Cytotoxicity profile of **apMUC1-MSNs** in MDA-MB-231 (grey bars) and MDA-MB-231-R (black bars). Cell viability study by WST-1 at 72 h in presence of different nanoparticle dosages. Data represent means ± SEM ($n = 3$).

Chemistry–A European Journal

Full Paper
doi.org/10.1002/chem.202001579

Chemistry
Europe
European Chemical
Societies Publishing

S63845 ratio used when loading the nanoparticles. The APTES and apMUC1 content were also determined (see Table S3).

Cargo controlled release and biocompatibility studies

To study the gating capacity of the MUC1 aptamer, we performed studies of rhodamine B delivery from **apMUC1-MSNs(RhB)** in the presence of a deoxyribonuclease I (DNAse I). Uncapping, due to hydrolysis of the capping apMUC1 aptamer by DNAse I, and subsequent payload delivery from **apMUC1-MSNs(RhB)** was monitored by following the fluorescence emission of rhodamine B at 572 nm ($\lambda_{exc} = 555$ nm) in the solution at scheduled times (Figure 1 B). There was low cargo release from **apMUC1-MSNs(RhB)** in the absence of DNAse I (less than 20% of the total delivery observed after 60 min), which demonstrates the correct blockage of the pores. However, a marked cargo release was detected in the presence of DNAse I. Hence, apMUC1 efficiently prevents premature delivery of the cargo from the capped nanoparticles.

To study the biocompatibility of the apMUC1-capped MSNs, the triple-negative breast cancer cell line MDA-MB-231 and the corresponding navitoclax resistant cell line, MDA-MB-231-R

(vide infra), were incubated with different concentrations of apMUC1-MSNs ($0-200$ μg mL^{-1}) for 72 h. Cell viability was kept around 80%, even at concentrations up to 200 μg mL^{-1} (Figure 1C). These results demonstrated that MUC1-gated MSNs are not toxic in TNBC cell lines.[26,53]

Targeted cellular uptake studies

As previously stated, the nanoparticles are capped with an aptamer designed to target the MUC1 surface protein, which has been reported to be overexpressed in BC cell lines.[56,57] To carry out targeting studies, we first created a TNBC cell line model resistant to navitoclax (MDA-MB-231-R) by treating MDA-MB-231 cells with a constant concentration of navitoclax for two months. Then, we demonstrated that MUC1 expression is found in both MDA-MB-231 and MDA-MB-231-R cell lines (Figure 2 A). In a second step, the targeting ability of **apMUC1-MSNs(RhB)** was demonstrated with cell internalization studies of this solid and nanoparticles capped with a random aptamer (**apRandom-MSNs(RhB)**) in MDA-MB-231 and MDA-MB-231-R cells by flow cytometry and confocal microscopy. Both cell lines showed a clear increase of RhB fluorescence signal inside
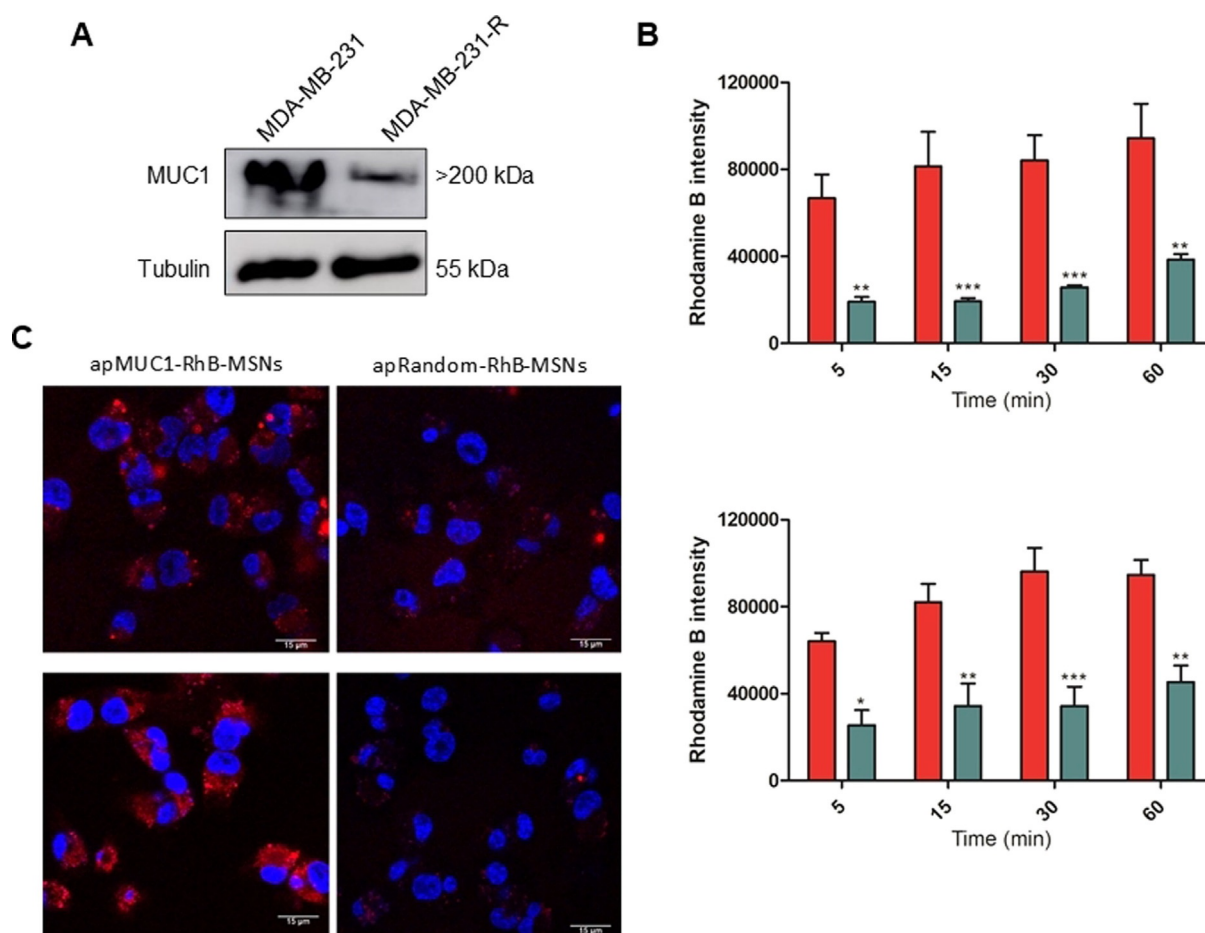

Figure 2. A) Western blot analysis of MUC1 expression in MDA-MB-231 and MDA-MB-231-R. B) Fluorescence intensity kinetic of MDA-MB-231 cells (top graph) and MDA-MB-231-R (bottom graph) analyzed by flow cytometry after treatment with **apMUC1-MSNs(RhB)** (red bars) or **apRandom-MSNs(RhB)** (grey bars). Data represent the means ± SEM of at least three independent experiments. C) Confocal images of nanoparticles uptake by MDA-MB-231 (top panel) and MDA-MB-231-R (bottom panel) in presence of **apMUC1-MSNs(RhB)** (left) or **apRandom-MSNs(RhB)** (right) after 3 h of treatment with the nanoparticles.

Chemistry–A European Journal

Full Paper
doi.org/10.1002/chem.202001579

Chemistry Europe
European Chemical
Societies Publishing

the cells over time when treated with **apMUC1-MSNs(RhB)**, whereas a remarkable weaker fluorescence intensity was observed in cells when treated with **apRandom-MSNs(RhB)** (Figure 2B).

The role played by the apMUC1 aptamer in the preferential internalization of **apMUC1-MSNs(RhB)** was also assessed by confocal microscopy. A larger emission signal of rhodamine B was detected in cells treated with **apMUC1-MSNs(RhB)** when compared with those incubated with **apRandom-MSNs(RhB)** (Figure 2C). These results demonstrate the targeting ability of **apMUC1-MSNs(RhB)** to TNBC cell lines, as a consequence of the selective interaction between the capping apMUC1 aptamer and the MUC1 receptor in the cell membrane.

Navitoclax resistance overcoming in TNBC cells

As stated above it was in our aim to develop nanoparticles able to overcome navitoclax resistance in TNBC cells by using apMUC1-capped nanoparticles loaded with both navitoclax and the highly selective Mcl-1 inhibitor S63845. To carry out this study we created, as stated above, a TNBC cell line model resistant to navitoclax (MDA-MB-231-R) by treating MDA-MB-231 cells with navitoclax for two months. Protein characterization confirmed that treatment with navitoclax produced Mcl-1 overexpression in MDA-MB-231-R (Figure 3 A). Resistance to navitoclax was confirmed in dose-response assays, which demonstrated that navitoclax IC_{50} increased from 2 μM in MDA-MB-231 to 17 μM in MDA-MB-231-R (Figure 3B). Then, MDA-MB-231 cells were treated with **apMUC1-MSNs, apMUC1-MSNs(S63845), apMUC1-MSNs(Nav), apMUC MSNs(Nav/S63845, 10:1)** and **apMUC1-MSNs(Nav/S63845, 2:1)** (25 μg mL^{-1}) and cell viability was determined by WST-1 assay (Figure 4A, left). A statistically significant cell viability reduction was observed in MDA-MB-231 cell line for all the nanoparticles containing navitoclax (i.e., **apMUC1-MSNs(Nav), apMUC1-MSNs(Nav/S63845, 10:1)** and **apMUC1-MSNs(Nav/S63845, 2:1)**), as the MDA-MB-231 cell line is sensitive to navitoclax. In contrast, the treatment of the navitoclax-resistant MDA-MB-231-R cell line with **apMUC1-MSNs(Nav)** resulted in no change

in viability (Figure 4A, right) compared with the control (untreated cells). Viability of the cell line MDA-MB-231-R was neither affected upon treatment with the nanoparticles only containing the Mcl-1 inhibitor S63845 (i.e., **apMUC1-MSNs(S63845)**). As a clear contrast, a remarkable cell viability reduction to 30%, when compared with the untreated control (see also Figure 4A, right), was found for MDA-MB-231-R cells treated with the nanocarriers loaded with both navitoclax and S63845 drugs (i.e. **apMUC1-MSNs(Nav/S63845, 10:1)** and **apMUC1-MSNs(Nav/S63845, 2:1)**). The results obtained clearly indicate that apMUC1-gated nanocarriers can be used not only for TNBC cell apoptosis induction by releasing BH3 mimetic drugs (i.e., navitoclax), but also for killing navitoclax-resistant TNBC cells when navitoclax is combined in the same nanoparticle with the Mcl-1 inhibitor S63845. This result, together with the targeting ability of the nanoparticles to the membrane protein MUC1 overexpressed in TNBC cells (vide ante), makes these nanodevices functional potential candidates to treat triple-negative breast cancer.

Platelets protection assay

Preclinical and clinical studies have shown that navitoclax exhibits therapeutic effect against different malignancies. Nevertheless, thrombocytopenia is the major adverse effect of this drug and the main reason why navitoclax clinical use has not been approved.[58–60] Severe thrombocytopenia in preclinical animal models and patients is caused by Bcl-xL inhibition in platelets, which dramatically reduces platelet lifespan.[58,59,61,62] In order to study platelet protection from thrombocytopenia due to navitoclax encapsulation, human complete blood cell extract was treated with **apMUC1-MSNs(Nav)** and the free drug at equivalent doses. Also, blood samples were treated with **apMUC1-MSNs** as a nontoxicity control. As expected, **apMUC1-MSNs** scaffold did not induce apoptosis in platelets (Figure S2). Moreover, we found that navitoclax encapsulation in **apMUC1-MSNs(Nav)** protected platelets from apoptosis since annexin V levels were significantly lower when platelets were treated with the encapsulated drug, in comparison to the
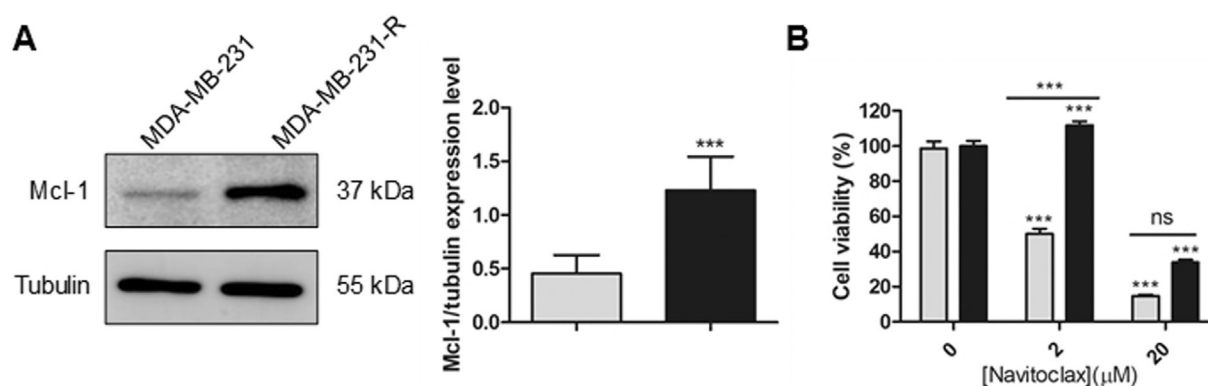

Figure 3. A) Western blot analysis of Mcl-1 expression in MDA-MB-231 (grey bar) and MDA-MB-231-R (black bar). Data represent means ± SEM ($n = 6$). Statistical significance was determined by the t Student test (*** $p < 0.001$). B) Navitoclax cytotoxicity evaluation in MDA-MB-231 (grey bars) and MDA-MB-231-R (black bars). Data represent means ± SEM ($n = 3$). Statistical significance was determined by one-way ANOVA and Tukey post-test (*** $p < 0.001$).
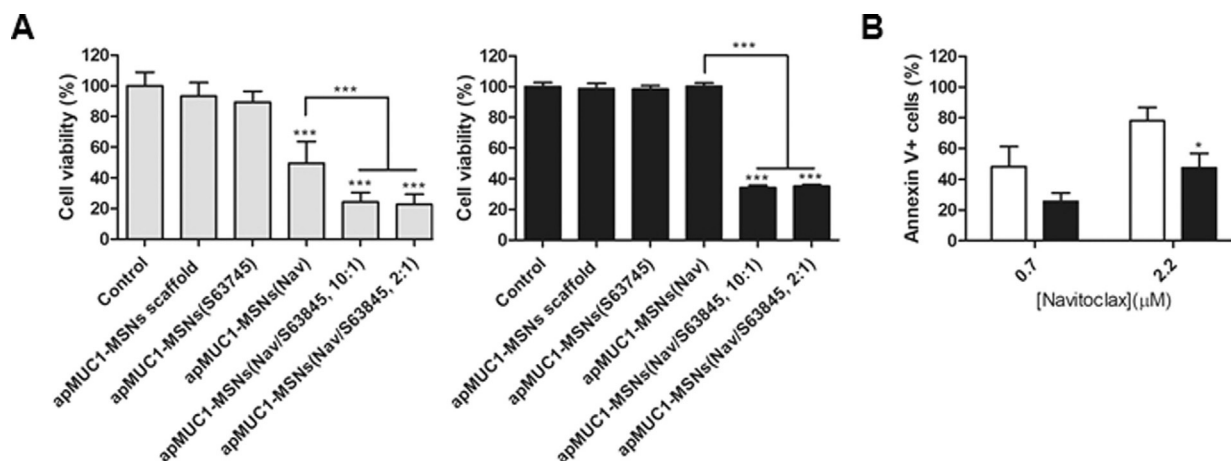
Chemistry–A European Journal

Full Paper
doi.org/10.1002/chem.202001579

Chemistry Europe
European Chemical
Societies Publishing

Figure 4. A) Cell viability analysis by WST-1 assay in MDA-MB-231 (left) and MDA-MB-231-R (right) incubated with apMUC1-gated MSNs at 25 $\mu g\,mL^{-1}$ for 72 h. Data represent means $\pm$ SEM ($n=3$). Statistically significance was determined by one-way ANOVA and Tukey post-test (*** $p < 0.001$). B) Thrombocytopenia induced by navitoclax in platelets. Human blood complete extract was treated with free navitoclax (white bar) and encapsulated navitoclax in **apMUC1-MSNs(Nav)** (black bar). Platelet apoptosis was measured by annexin V assay assessed by flow cytometry ($n=4$). Statistically significance was determined by two-way ANOVA (*** $p < 0.001$).

free drug (Figure 4 B). These results demonstrate that MSNs navitoclax encapsulation protects platelets from apoptosis induced by Bcl-xL inhibition. This suggests that the encapsulation of navitoclax can be a suitable potential strategy to widen the therapeutic window of navitoclax and other drugs, whose clinical applications have been limited because of secondary effects.[63–66]

Conclusions

In summary, we report herein a multifunctional nanodevice capable of overcoming navitoclax resistance in TNBC by the co-delivery of navitoclax and the Mcl-1 inhibitor S63845. Nanoparticles consist of MSNs loaded with navitoclax and S63845 or a combination of both drugs, functionalized with APTES and capped with the apMUC1-targeting aptamer. Nanoparticles loaded with rhodamine B are also prepared. The nanodevice loaded with rhodamine (i.e., **apMUC1-MSNs(RhB)**) remains capped in a buffer solution, yet the payload is delivered on-command upon apMUC1 hydrolysis by DNAse I. Flow cytometry and confocal microscopy studies carried out in TNBC cells revealed that nanoparticles **apMUC1-MSNs(RhB)** are preferentially internalized in TNBC cells when compared with nanoparticles capped with a random aptamer. Furthermore, the nanoparticles loaded with both drugs (i.e. **apMUC1-MSNs(Nav/S63845)**) can overcome navitoclax resistance in TNBC cell lines, that overexpress Mcl-1 antiapoptotic protein as a resistance mechanism. Besides, navitoclax encapsulation in MSNs demonstrates to effectively protect platelets from apoptosis. This promising result suggested that the encapsulation of navitoclax can wide up its horizons in clinical application, the use of which has been limited because of the induction of thrombocytopenia in patients. Moreover, we demonstrate that targeted-delivery of navitoclax and S63845 using apMUC1-gated mesoporous silica nanoparticles is an attractive strategy for specific drug release in TNBC cells by taking the advantage of

the active targeting of the engineered MSNs while increasing the treatment efficacy and reducing drug side effects. These results point MSNs as versatile platforms for the simultaneous controlled delivery of multiple chemotherapeutic agents as a synergistic treatment to overcome drug resistance in tumors, which still is an uncover need within the biomedical field.[66–69]

Experimental Section

Synthesis of the mesoporous silica nanodevices

In a typical synthesis procedure,[70] CTAB (1.00 g, 2.74 mmol) was dissolved in 480 mL of deionized water before adding a solution of NaOH (3.5 mL, 2.00 M). The temperature was adjusted at 80 °C and then TEOS (5.00 mL, 2.57×10^{-2} mol) was added dropwise to the surfactant solution. The final solution was stirred for 2 h to give a white precipitate. The solid was isolated by centrifugation-washing cycles of 20 min at $15\,000 \times g$ in deionized water until pH 7 was reached. The material was dried at 60 °C and the final solid was calcined (Mufla Furnace) at 550 °C in an oxidant atmosphere to remove the template phase, obtaining the mesoporous scaffold (MSNs).

Synthesis of APTES-MSNs(RhB)

The pores of the calcined MSNs were loaded with rhodamine B. For this purpose, MSNs (300 mg) were suspended in an acetonitrile solution containing rhodamine B (57.5 mg, 0.4 mmol g^{-1} solid) and stirred for 48 h. Then, an excess of (3-aminopropyl) triethoxysilane (APTES, 0.59 µL, 2.5 mmol) was added to the mixture and stirred for 5.5 h at room temperature. Finally, the solid was isolated by centrifugation and dried at 37 °C to yield a pink solid.

Synthesis of apMUC1-MSNs(RhB)

The MUC1-targeting aptamer (apMUC1) (5'-GCA GTT GAT CCT TTG GAT ACC CTG G-3') was electrostatically adsorbed onto the external surface of **APTES-MSNs(RhB)**. In this respect, **APTES-MSNs(RhB)** (1 mg) were suspended in PBS and mixed with apMUC1 (150 µL,

Chemistry–A European Journal

Full Paper
doi.org/10.1002/chem.202001579

Chemistry Europe
European Chemical
Societies Publishing

100 μm). The mixture was stirred at 37°C for 30 min and then nanoparticles were centrifuged and washed with PBS to get the final solid **apMUC1-MSNs(RhB)**. **APTES-MSNs(RhB)** were also coated with a MUC1 non-targeting aptamer (apRandom) (5′-AAG CAC TTT CAG TGG GGA GGA GGG TTG ATA GGT TAA GAG-3′), that was employed as a negative control in the targeting study, obtaining the nanoparticles referred as **apRandom-MSNs(RhB)**.

Synthesis of drug-loaded apMUC1-gated MSNs

We aimed to overcome navitoclax resistance in a TNBC cell model using navitoclax and the Mcl-1 inhibitor S63845 combination of drugs encapsulated in MSNs. For this purpose, calcined MSNs (20 mg) were mixed with 15 mg (0.015 mmol) of navitoclax (**apMUC1-MSNs(Nav)**) and 13 mg (0.015 mmol) of S63845 (**apMUC1-MSNs(S63845)**), obtaining single drug-loaded nanoparticles as nontoxicity controls in the navitoclax resistant cell line. In addition, MSNs were mixed with a combination of navitoclax and the Mcl-1 inhibitor S63845: 20 mg of MSNs were mixed with 14 mg (0.015 mmol) of navitoclax plus 1.2 mg S63845 (0.0015 mmol) of S63845 to obtain **apMUC1-MSNs(Nav/S634845, 10:1)**, and also with 10.3 mg (0.015 mmol) of navitoclax plus 4.4 mg (0.005 mmol) of S63845 to obtain **apMUC1-MSNs(Nav/S63845, 2:1)**. Mixtures were suspended in dichloromethane and stirred for 48 h at room temperature in an argon atmosphere to achieve maximum loading in the pores of the MCM-41 scaffolding. Afterward, 39 μL (0.16 mmol) of APTES was added to the solution and the suspension was stirred for 5.5 h. Finally, solids were isolated by vacuum filtration and dried overnight under vacuum flux, giving the set of nanoparticles used to overcome navitoclax resistance in TNBC cells (Table S1).

Standard characterization procedures of the prepared materials

Powder X-ray diffraction (PXRD), transmission electron microscopy (TEM), TEM-EDX, N_2 adsorption-desorption isotherms, Fourier-transform infrared spectroscopy (FTIR) and nuclear magnetic resonance (NMR) were employed for materials characterization. PDRX measurements were taken on Seifert 3000TT diffractometer using CuKα radiation. TEM images were acquired under Philips CM-10 that worked at 100 kV. TEM-EDX imaging was carried out using a JEOL JEM-2100 LaB6 electron microscope working at 200 kV accelerating voltage and equipped with an Oxford Instruments INCA x-sight (Si(Li) detector) and a Zeiss SESAM microscope (200 kV) equipped with an energy dispersive X-ray (EDX) spectroscopy system from ThermoFisher. The N_2 adsorption–desorption isotherms were recorded in a Micromeritics TriStar II Plus automated analyzer. FTIR measurements were taken by Bruker Tensor 27 spectrometer. ^{1}H and ^{13}C NMR spectra were recorded on a Bruker FT-NMR Avance 400 (Ettlingen, Germany) spectrometer at 300 K, using TMS as an internal standard. ζ potential was determined from the particle mobility values by applying the Smoluchwski model in a Malvern Zetasizer ZS instrument. Fluorescence measured was recorded by a JASCO FP-8500 spectrophotometer. Cell viability measurements were taken in a Wallac 1420 workstation. Confocal microscopy imaging was performed with a Leica TCS SP8 HyVolution II (Leica Microsystems Heidelberg GmbH) inverted laser scanning confocal microscope. Confocal image analysis was carried out with ImageJ software. Flow cytometry experiments were performed CytoFLEX S equipped with 4 lasers and 13 fluorescence detectors (Beckman-Coulter, USA) and data analysis with CytExpert Software.

Cargo delivery studies

To check the proper working of the capping aptamer, **apMUC1-MSNs(RhB)** were suspended in buffer solution (20 mM Tris-HCl, 37.5 mM MgCl₂, pH 7.5) or buffer solution plus DNAse I (1 mg mL⁻¹). In a typical experiment, 1 mg of **apMUC1-MSNs(RhB)** was suspended in 1 mL of buffer solution or 1 mL of buffer solution containing DNAse I and stirred at 37°C for 60 min. At certain times aliquots were taken and centrifuged to remove the solid. Rhodamine B delivery was determined by measuring its fluorescence at 572 nm (λ_{ex} = 555 nm).

Cell culture conditions

Triple-negative breast cancer cells (MDA-MB-231) were purchased from ATCC and grown in Dulbecco's Modified Eagle Medium (DMEM)-high glucose supplemented with 10% of fetal bovine (FBS). Cells were incubated at 37°C in a 5% CO₂ atmosphere and 95% air. For navitoclax resistance induction, MDA-MB-231 were incubated with navitoclax for two months in 100 mm cell culture dishes. DMEM medium containing navitoclax was weekly replaced. Finally, MDA-MB-231 resistant to navitoclax (MDA-MB-231-R) were obtained.

Protein expression characterization by Western blot

Mcl-1 and MUC1 expression in the TNBC cell lines were studied by Western blot. For this purpose, MDA-MB-231 and MDA-MB-231-R cell lines were grown to confluence. For Mcl-1 expression characterization whole-cell extracts were obtained by scraping the cell monolayer using buffer lysis composed by 25 mM Tris-HCl, pH 7.4, 1 mM EDTA, 1 mM EGTA and 1% SDS, plus protease and phosphatase inhibitors. Lysates were resolved by Western blot (12% SDS-PAGE). For MUC1 expression characterization, cells were trypsinized and washed with PBS. Then cells were incubated with RIPA buffer, composed by 10 mM Tris-Cl (pH 8.0), 1 mM EDTA, 1% Triton X-100, 0.1% sodium deoxycholate, 0.1% SDS, 140 mM NaCl and 1 mM PMSF, for 30 min at 4°C under shaking. Lysates were separated by Western blot (6% SDS-PAGE). After the Western blot gel run, proteins were electrophoretically transferred to nitrocellulose membranes and blocked with nonfat milk 5%. Then membranes were washed with 0.1% Tween/TBS and incubated overnight with primary antibodies: anti-Mcl-1 (#4572) (*Cell Signalling*) and anti-MUC1 (VU4H5) (#4538) (*Cell Signalling*). α-Tubulin was used as reference control: anti-tubulin (ab6160) (Abcam). Membranes were washed and incubated with horseradish peroxidase-conjugated secondary antibodies for chemiluminescence detection in Amersham Imager 600 equipment.

Cytotoxicity cell studies with apMUC1-MSNs

The biocompatibility of **apMUC1-MSNs** was studied in MDA-MB-231 and MDA-MB-231-R. The cytotoxic effect was evaluated by WST-1 assay. TNBC cell lines were seed in 96-well plates at 10000 cells per well confluence one day before treatment. Then cells were treated with different concentrations of **apMUC1-MSNs** (0, 25, 50, 100 and 200 μg mL⁻¹) for 72 h. After that incubation time with the nanoparticles, WST-1 was added to each well and absorbance was measured at 450 at Wallace 1420 workstation.

Navitoclax resistance overcoming TNBC cells

The proper navitoclax sensitizing activity of the nanoparticles was evaluated in MDA-MB-231-R. TNBC cells were seeded in 96-well plates at 10000 cells per well and incubated with **apMUC1-**

MSNs(Nav), **apMUC1-MSNs(S63845)**, **apMUC1-MSNs(Nav/S63845, 10:1)** and **apMUC1-MSNs(Nav/S63845, 2:1)** at 25 µg mL⁻¹ for 72 h. MDA-MB-231 was also treated with the set of the prepared nanoparticles at the same conditions. Cell viability was assessed by WST-1 assay; 10 µL per well of WST-1 were added and incubated for approximately one hour. Then absorbance was measured at 595 nm.

Targeted cellular uptake studies

The targeting properties of the prepared nanodevices were studied in MDA-MB-231 and MDA-MB-231-R. To this aim, MSNs loaded with rhodamine B and capped with a MUC1 non-targeting random aptamer (**apRandom-MSNs(RhB)**) were prepared as a control to follow the selective targeting of **apMUC1-MSNs(RhB)**. Firstly, cellular uptake was studied by flow cytometry in TNBC cells. For this purpose, MDA-MB-231 and MDA-MB-231-R were seeded on 6-well plates at 300000 cells per well 1 day before treatment. Cells were incubated with **apMUC1-MSNs(RhB)** and **apRandom-MSNs(RhB)** at 25 µg mL⁻¹ for 30 min and washed with PBS to remove the non-internalized nanoparticles. Finally, the cells were incubated for a total time of 1 h in the presence of the nanodevices. Then, the cells were trypsinized and collected for rhodamine B quantification by flow cytometry. The single-cell fluorescence measurements were performed in CytoFLEX S (Beckman-Coulter, USA) equipped with 4 lasers and 13 fluorescence detectors and analyzed in the CytoFLEX software. Additionally, nanoparticles' internalization was followed by confocal microscopy. The cells were seeded on glass coverslips in 6-well plates at 800000 cells per well and incubated 24 h at 37°C. Cells were treated with **apMUC1-MSNs(RhB)** and **apRandom-MSNs(RhB)** (25 µg mL⁻¹) for 30 min. Then cells were washed with PBS and fresh media was added until complete 3 h of incubation with the nanoparticles. Finally, cell nuclei were stained with Hoechst 33342 (2 µg mL⁻¹) and fluorescence intensity was monitored through a Leica TCS SP8 confocal microscope.

Platelets protection assay

For human platelet apoptosis assay, blood from three healthy volunteers was extracted according to the UPV ethics procedures. Navitoclax's main side effect is the induction of thrombocytopenia in patients when treated in clinical phases. To demonstrate that navitoclax encapsulation in the nanodevices protects platelets against apoptosis, human complete blood extract was incubated with **apMUC1-MSNs(Nav)** and with equivalent dosages of the free navitoclax for 4 h. **apMUC1-MSNs** was added, with equivalent dosages of **apMUC1-MSNs(Nav)**, to discard the toxicity of the MSNs scaffold. Platelets were stained with the pan-platelet antibody CD41/phycoerythrin (Invitrogen) and apoptosis level was determined by annexin V/FITC labeling (Immunostep). Platelet apoptosis was determined by flow cytometry in a CytoFLEX S (Beckman-Coulter, USA).

Conflict of interest

The authors declare no conflict of interest.

Keywords: apoptosis · cancer · drug delivery · nanoparticles · targeting

[1] F. Bray, J. Ferlay, I. Soerjomataram, R. L. Siegel, L. A. Torre, A. Jemal, *Cancer J. Clin.* **2018**, *68*, 394–424.
[2] Globocan, *Globoscan* **2018**, *947*, 2018.
[3] G. Turashvili, E. D. Lightbody, K. Tyryshkin, S. K. SenGupta, B. E. Elliott, Y. Madarnas, A. Ghaffari, A. Day, C. J. B. Nicol, *FASEB J.* **2018**, *32*, 5937–5954.
[4] J. Collignon, L. Lousberg, H. Schroeder, G. Jerusalem, *Breast Cancer* **2016**, *8*, 93–107.
[5] X. Dai, T. Li, Z. Bai, Y. Yang, X. Liu, J. Zhan, B. Shi, *Am. J. Cancer Res.* **2015**, *5*, 2929–2943.
[6] H. A. Wahba, H. A. El-Hadaad, *Cancer Biol. Med.* **2015**, *12*, 106–116.
[7] H. Li, L. Liu, H. Chang, Z. Zou, D. Xing, *Cell Death Dis.* **2018**, *9*, 137.
[8] X. Dai, L. Xiang, T. Li, Z. Bai, *J. Cancer* **2016**, *7*, 1281–1294.
[9] J. T. Opferman, *FEBS J.* **2016**, *283*, 2661–2675.
[10] H. Kalkavan, D. R. Green, *Cell Death Differ.* **2018**, *25*, 46–55.
[11] M. C. Wei, W. X. Zong, E. H. Y. Cheng, T. Lindsten, V. Panoutsakopoulou, A. J. Ross, K. A. Roth, G. R. Macgregor, C. B. Thompson, S. J. Korsmeyer, *Science* **2001**, *292*, 727–730.
[12] B. Wang, Z. Ni, X. Dai, L. Qin, X. Li, J. Xu, J. Lian, F. He, *Mol. Cancer* **2014**, *13*, 1–11.
[13] J. Belmar, S. W. Fesik, *Pharmacol. Ther.* **2015**, *145*, 76–84.
[14] *Cancer. Gov.* **2019**, 1–2.
[15] A. Kaefer, J. Yang, P. Noertersheuser, S. Mensing, R. Humerickhouse, W. Awni, H. Xiong, *Cancer Chemother. Pharmacol.* **2014**, *74*, 593–602.
[16] K. Louault, T. L. Bonneaud, C. Séveno, P. Gomez-Bougie, F. Nguyen, F. Gautier, N. Bourgeois, D. Loussouarn, O. Kerdraon, S. Barillé-Nion, P. Jézéquel, M. Campone, M. Amiot, P. P. Juin, F. Souazé, *Oncogene* **2019**, *38*, 3261–3273.
[17] K. J. Campbell, S. Dhayade, N. Ferrari, A. H. Sims, E. Johnson, S. M. Mason, A. Dickson, K. M. Ryan, G. Kalna, J. Edwards, S. W. G. Tait, K. Blyth, *Cell Death Dis.* **2018**, *9*, 19.
[18] A. Kotschy, Z. Szlavik, J. Murray, J. Davidson, A. L. Maragno, G. Le Toumelin-Braizat, M. Chanrion, G. L. Kelly, J. N. Gong, D. M. Moujalled, A. Bruno, M. Csekei, A. Paczal, Z. B. Szabo, S. Sipos, G. Radics, A. Proszenyak, B. Balint, L. Ondi, G. Blasko, A. Robertson, A. Surgenor, P. Dokurno, I. Chen, N. Matassova, J. Smith, C. Pedder, C. Graham, A. Studeny, G. Lysiak-Auvity, A. M. Girard, F. Gravé, D. Segal, C. D. Riffkin, G. Pomilio, L. C. A. Galbraith, B. J. Aubrey, M. S. Brennan, M. J. Herold, C. Chang, G. Guasconi, N. Cauquil, F. Melchiore, N. Guigal-Stephan, B. Lockhart, F. Colland, J. A. Hickman, A. W. Roberts, D. C. S. Huang, A. H. Wei, A. Strasser, G. Lessene, O. Geneste, *Nature* **2016**, *538*, 477–482.
[19] D. Merino, J. R. Whittle, F. Vaillant, A. Serrano, J. N. Gong, G. Giner, A. L. Maragno, M. Chanrion, E. Schneider, B. Pal, X. Li, G. Dewson, J. Gräsel, K. Liu, N. Lalaoui, D. Segal, M. J. Herold, D. C. S. Huang, G. K. Smyth, O. Geneste, G. Lessene, J. E. Visvander, G. J. Lindeman, *Sci. Transl. Med.* **2017**, *9*, eaam7049.
[20] Z. Li, S. He, A. T. Look, *Leukemia* **2019**, *33*, 262–266.
[21] Y. Barenholz, *J. Controlled Release* **2012**, *160*, 117–134.
[22] J. Wolfram, M. Zhu, Y. Yang, J. Shen, E. Gentile, D. Paolino, M. Fresta, G. Nie, C. Chen, H. Shen, M. Ferrari, Y. Zhao, *Curr. Drug Targets* **2015**, *16*, 1671–1681.
[23] M. Yu, Z. Gu, T. Ottewell, G. Yu, *J. Mater. Chem. B* **2017**, *5*, 3241–3252.
[24] J. Fang, H. Nakamura, H. Maeda, *Adv. Drug Delivery Rev.* **2011**, *63*, 136–151.
[25] J. Lu, M. Liong, Z. Li, J. I. Zink, F. Tamanoi, *Small* **2010**, *6*, 1794–1805.
[26] M. Y. Hanafi-Bojd, S. A. Moosavian Kalat, S. M. Taghdisi, L. Ansari, K. Abnous, B. Malaekeh-Nikouei, *Drug Dev. Ind. Pharm.* **2018**, *44*, 13–18.

[27] Y. Wang, Q. Zhao, N. Han, L. Bai, J. Li, J. Liu, E. Che, L. Hu, Q. Zhang, T. Jiang, S. Wang, *Nanomed. Nanotechnol. Biol. Med.* **2015**, *11*, 313 – 327.

[28] Y. Yang, C. Yu, *Nanomedicine* **2016**, *12*, 317 – 332.

[29] S. Zhao, M. Xu, C. Cao, Q. Yu, Y. Zhou, J. Liu, *J. Mater. Chem. B* **2017**, *5*, 6908 – 6919.

[30] P. Pei, F. Yang, J. Liu, H. Hu, X. Du, N. Hanagata, S. Zhao, Y. Zhu, *Biomater. Sci.* **2018**, *6*, 1414 – 1423.

[31] J. Florek, R. Caillard, F. Kleitz, *Nanoscale* **2017**, *9*, 15252 – 15277.

[32] F. Farjadian, A. Roointan, S. Mohammadi-Samani, M. Hosseini, *Chem. Eng. J.* **2019**, *359*, 684 – 705.

[33] V. Mamaeva, C. Sahlgren, M. Lindén, *Adv. Drug Delivery Rev.* **2013**, *65*, 689 – 702.

[34] S.-H. Wu, C.-Y. Mou, H.-P. Lin, *Chem. Soc. Rev.* **2013**, *42*, 3862 – 3875.

[35] a) E. Aznar, M. Oroval, J. R. Murgía, R. Martínez-Máñez, F. Sancenón, *Chem. Rev.* **2016**, *116*, 561 – 718; b) E. Aznar, C. Coll, M. D. Marcos, R. Martínez-Máñez, F. Sancenón, J. Soto, P. Amorós, J. Cano, E. Ruiz, *Chem. Eur. J.* **2009**, *15*, 6877 – 6888; c) E. Aznar, R. Villalonga, C. Giménez, F. Sancenón, M. D. Marcos, R. Martínez-Máñez, P. Díez, J. M. Pingarrón, P. Amorós, *Chem. Commun.* **2013**, *49*, 6391 – 6393; d) L. Mondragón, N. Mas, V. Ferragud, C. de la Torre, A. Agostini, R. Martínez-Máñez, F. Sancenón, P. Amorós, E. Pérez-Payá, M. Orzáez, *Chem. Eur. J.* **2014**, *20*, 5271 – 5281; e) C. Giménez, C. de la Torre, M. Gorbe, E. Aznar, F. Sancenón, J. R. Murguía, R. Martínez-Máñez, M. D. Marcos, P. Amorós, *Langmuir* **2015**, *31*, 3753 – 3762; f) A. Llopis-Lorente, B. Lozano-Torres, A. Bernardos, R. Martínez-Máñez, F. Sancenón, *J. Mater. Chem. B* **2017**, *5*, 3069 – 3083; g) A. García-Fernández, E. Aznar, R. Martínez-Máñez, F. Sancenón, *Small* **2020**, *16*, 1902242.

[36] H. Mekaru, J. Lu, F. Tamanoi, *Adv. Drug Delivery Rev.* **2015**, *95*, 40 – 49.

[37] K. Möller, T. Bein, *Chem. Mater.* **2017**, *29*, 371 – 388.

[38] J. Wen, K. Yang, F. Liu, H. Li, Y. Xu, S. Sun, *Chem. Soc. Rev.* **2017**, *46*, 6024 – 6045.

[39] J. G. Croissant, Y. Fatieiev, A. Almalik, N. M. Khashab, *Adv. Healthcare Mater.* **2018**, *7*, 1 – 75.

[40] C. Argyo, V. Weiss, C. Bräuchle, T. Bein, *Chem. Mater.* **2014**, *26*, 435 – 451.

[41] J. Zhu, Y. Niu, Y. Li, Y. Gong, H. Shi, Q. Huo, Y. Liu, Q. Xu, *J. Mater. Chem. B* **2017**, *5*, 1339 – 1352.

[42] W. Q. Lim, S. Z. F. Phua, H. V. Xu, S. Sreejith, Y. Zhao, *Nanoscale* **2016**, *8*, 12510 – 12519.

[43] S. M. Nimjee, C. P. Rusconi, B. A. Sullenger, *Annu. Rev. Med.* **2005**, *56*, 555 – 583.

[44] F. J. Hernandez, L. I. Hernandez, A. Pinto, T. Schäfer, V. C. Özalp, *Chem. Commun.* **2013**, *49*, 1285 – 1287.

[45] N. Poonia, V. Lather, D. Pandita, *Drug Discovery Today* **2018**, *23*, 315 – 332.

[46] R. Bazak, M. Houri, S. El Achy, S. Kamel, H. Officer, T. Refaat, N. Medicine, R. H. Lurie, *J. Cancer Res. Clin. Oncol.* **2015**, *141*, 769 – 784.

[47] S. Vandghanooni, J. Barar, M. Eskandani, Y. Omidi, *TrAC Trends Anal. Chem.* **2020**, *123*, 115759.

[48] W. Alshaer, H. Hillaireau, J. Vergnaud, S. Mura, C. Deloménie, F. Sauvage, S. Ismail, E. Fattal, *J. Controlled Release* **2018**, *271*, 98 – 106.

[49] X. Xie, F. Li, H. Zhang, Y. Lu, S. Lian, H. Lin, Y. Gao, L. Jia, *Eur. J. Pharm. Sci.* **2016**, *83*, 28 – 35.

[50] Y. Shen, M. Li, T. Liu, J. Liu, Y. Xie, J. Zhang, S. Xu, H. Liu, *Int. J. Nanomed.* **2019**, *14*, 4029 – 4044.

[51] Y. Yang, W. Zhao, W. Tan, Z. Lai, D. Fang, L. Jiang, C. Zuo, N. Yang, Y. Lai, *Nanoscale Res. Lett.* **2019**, *14*, 390.

[52] M. S. Nabavinia, A. Gholoobi, F. Charbgoo, M. Nabavinia, M. Ramezani, K. Abnous, *Med. Res. Rev.* **2017**, *37*, 1518 – 1539.

[53] L. Pascual, C. Cerqueira-Coutinho, A. García-Fernández, B. de Luis, E. S. Bernardes, M. S. Albernaz, S. Missailidis, R. Martínez-Máñez, R. Santos-Oliveira, M. Orzaez, F. Sancenón, *Nanomed. Nanotechnol. Biol. Med.* **2017**, *13*, 2495 – 2505.

[54] J. G. Kelly, P. L. Martin-Hirsch, F. L. Martin, *Anal. Chem.* **2009**, *81*, 5314 – 5319.

[55] R. J. Speedy, *Biophys. Chem.* **2003**, *104*, 477 – 488.

[56] R. Wang, L. Yang, S. Li, D. Ye, L. Yang, Q. Liu, Z. Zhao, Q. Cai, J. Tan, X. Li, *Med. Sci. Monit.* **2018**, *24*, 412 – 420.

[57] M. D. Walsh, S. M. Luckie, M. C. Cummings, T. M. Antalis, M. A. McGuckin, *Breast Cancer Res. Treat.* **1999**, *58*, 253 – 266.

[58] W. H. Wilson, O. A. O. Connor, M. S. Czuczman, S. LaCasce, J. F. Gerecitano, J. P. Leonard, A. Tulpule, K. Dunleavy, H. Xiong, Y. L. Chiu, Y. Cui, T. Busman, S. W. Elmore, S. H. Rosenberg, A. P. Krivoshik, S. H. Enschede, R. A. Humericjkhouse, *Lancet Oncol.* **2010**, *11*, 1149 – 1159.

[59] L. Gandhi, D. R. Camidge, M. R. De Oliveira, P. Bonomi, D. Gandara, D. Khaira, C. L. Hann, E. M. McKeegan, E. Litvinovich, P. M. Hemken, C. Dive, S. H. Enschede, C. Nolan, Y. L. Chiu, T. Busman, H. Xiong, A. P. Krivoshik, R. HUmerickhouse, G. I. Shapiro, C. M. Rudin, *J. Clin. Oncol.* **2011**, *29*, 909 – 916.

[60] C. Tse, A. R. Shoemaker, J. Adickes, M. G. Anderson, J. Chen, S. Jin, E. F. Johnson, K. C. Marsh, M. J. Mitten, P. Nimmer, L. Roberts, S. K. Tahir, Y. Xiao, X. Yang, H. Zhang, S. Fesik, S. H. Rosenberg, S. W. Elmore, *Cancer Res.* **2008**, *68*, 3421 – 3428.

[61] M. A. Debrincat, I. Pleines, M. Lebois, R. M. Lane, M. L. Holmes, J. Corbin, C. J. Vandenberg, W. S. Alexander, A. P. Ng, A. Strasser, *Cell Death Dis.* **2015**, *6*, e1721.

[62] S. M. Schoenwaelder, K. E. Jarman, E. E. Gardiner, M. Hua, J. Qiao, M. J. White, E. C. Josefsson, I. Alwis, A. Ono, A. Willcox, R. K. Andrews, K. D. Mason, H. H. Salem, D. C. S. Huang, B. T. Kile, A. W. Roberts, S. P. Jackson, *Blood* **2011**, *118*, 1663 – 1674.

[63] D. Muñoz-Espín, M. Rovira, I. Galiana, C. Giménez, B. Lozano-Torres, M. Paez-Ribes, S. Llanos, S. Chaib, M. Muñoz-Martín, A. C. Ucero, G. Garaulet, F. Mulero, S. G. Dann, T. van Arsdale, D. J. Shields, A. Bernardos, J. R. Murguía, R. Martínez-Máñez, M. Serrano, *EMBO Mol. Med.* **2018**, *10*, 1 – 18.

[64] L. Zhang, Y. Chen, Z. Li, L. Li, P. Saint-Cricq, C. Li, J. Lin, C. Wang, Z. Su, J. I. Zink, *Angew. Chem. Int. Ed.* **2016**, *55*, 2118 – 2121; *Angew. Chem.* **2016**, *128*, 2158 – 2161.

[65] D. Schmid, G. E. Jarvis, F. Fay, D. M. Small, M. K. Greene, J. Majkut, S. Spence, K. M. McLaughlin, K. D. McCloskey, P. G. Johnston, A. Kissenpfennig, D. G. Longley, C. J. Scott, *Cell Death Dis.* **2014**, *5*, e1454.

[66] M. Janicka, J. Gubernator, *Expert Opin. Drug Delivery* **2017**, *14*, 1059 – 1075.

[67] K. H. Chun, J. H. Park, S. Fan, *Adv. Exp. Med. Biol.* **2017**, *1026*, 59 – 104.

[68] X. Wang, H. Zhang, X. Chen, *Cancer Drug Res.* **2019**, *2*, 141 – 160.

[69] P. T. Yin, P. Pongkulapa, H. Y. Cho, J. Han, N. J. Pasquale, H. Rabie, J. H. Kim, J. W. Choi, K. B. Lee, *ACS Appl. Mater. Interfaces* **2018**, *10*, 26954 – 26963.

[70] Q. Cai, Z. S. Luo, W. Q. Pang, Y. W. Fan, X. H. Chen, F. Z. Cui, *Chem. Mater.* **2001**, *13*, 258 – 263.